JOURNAL OF AIRCRAFT
Vol. 37, No. 1, January–February 2000

Wind-Tunnel Techniques to Successfully Predict F/A-18E In-Flight Lift and Drag

P. W. Niewald* and S. L. Parker†
The Boeing Company, St. Louis, Missouri 63166-0516

F/A-18E/F program acquisition requirements put heavy emphasis on aircraft performance capabilities. It was crucial that preflight performance predictions provide an accurate representation of actual flight performance to secure timely program funding authorization and to control flight test costs. The basis for these predictions would be wind-tunnel lift and drag results. Commitment of substantial resources to the wind-tunnel program was required. Large, high-fidelity wind-tunnel models were tested in facilities that featured large, interference-free test sections. Computational fluid dynamics tools were fully integrated into the wind-tunnel plan to ensure high-quality test programs. The wind-tunnel techniques that were employed are discussed, and a successful correlation between preflight predictions and early flight results is presented.

Introduction

THE F/A-18E preflight wind-tunnel test program initially focused on aerodynamic configuration development and was followed by database documentation testing. During the configuration development phase, relatively small subscale models were utilized to permit low-cost evaluation of numerous configuration refinements in a small transonic test facility owned by the airframe manufacturer. Small model scales facilitated aggressive parametric testing of all configuration components, but sacrificed confidence in lift and drag results due to reduced fidelity.

When configuration development had matured, large, high-fidelity wind-tunnel models were developed to support verification and documentation testing. These models employed state-of-the-art instrumentation techniques and were tested in wind-tunnel facilities with large test sections and relatively high Reynolds number capability. Computational fluid dynamics (CFD) tools were also employed in the model design and test process to ensure the validity of test results. The combination of model fidelity, integrated CFD support, and test-facility capability produced a preflight aerodynamic database of unprecedented quality for tactical aircraft. This database was completed more than 1 year prior to first flight.

This paper highlights the techniques used to determine F/A-18E wind-tunnel lift and drag characteristics for the purpose of generating aircraft performance predictions. A successful correlation of wind-tunnel predicted lift and drag with early flight results is presented. A companion paper[1] highlights the successful flight test techniques.

Aircraft Description

The F/A-18E (see Fig. 1) is an upgraded follow-on to the F/A-18C Hornet strike fighter. It is a single-place, midwing, highly maneuverable, twin-engine fighter that, compared to its predecessor, offers greater range and endurance, the capability to carry heavier payloads, increased ability to bring unused high-value stores back to the carrier, and enhanced survivability.

Airframe

A stretched fuselage and larger wing provides expanded internal fuel volume, offering a substantial increase in mission radius and greater endurance for more time on station. The addition of two new wing store stations enhances mission flexibility, expanding loading options and increasing maximum external payload. The F/A-18E employs the same highly efficient aerodynamic design as the F/A-18C including a moderately swept wing with a highly swept leading-edge extension (LEX), wing-leading and trailing-edge maneuver flaps, a low-mounted horizontal tail, and canted vertical tails.

Propulsion System

The air induction system of the F/A-18E aircraft consists of two fixed-geometry, side fuselage mounted inlets. The inlets are 10-deg, dual-ramp external compression inlets located under the wing LEX. The induction system utilizes a partitioned passive bleed system to control the terminal shock/boundary-layer interaction. The engines are two General Electric F414-GE-400 augmented low-bypass, variable-exhaust nozzle geometry, twin-spool turbofans with afterburners. The F414-GE-400 engines are derived from the highly reliable F404 family in today's F/A-18C aircraft.

Flight Control System

The aircraft is controlled by a digital fly-by-wire flight control system through hydraulic flight control surfaces. Leading- and trailing-edge flap deflections are scheduled for best cruise and maneuver performance by effectively varying the wing camber. Lateral control is provided by a combination of ailerons, flaps, and asymmetric deflections of the all-movable horizontal tail. Pitch attitude is controlled by symmetric deflections of the horizontal tail surfaces. Dual rudders provide directional control. The F/A-18E incorporates a deflectable spoiler on the aft, upper surface of the LEX. Aerodynamic deceleration capability is derived from deflection of the ailerons, trailing-edge flaps, rudders, and LEX spoilers.

Wind-Tunnel Test Program

F/A-18E wind-tunnel testing in support of configuration development commenced in 1991. A 5% scale force and moment model was the workhorse for this effort. By late 1993 the configuration had matured, and a high-fidelity, 8% scale force and moment model was being fabricated. Documentation testing was conducted in 1994 with the 8% model and a 15% model that provided corrections for support-system effects. The preflight aerodynamic database was completed by fall 1994, approximately 1 year prior to first flight.

Wind-Tunnel Models

8% Scale Force and Moment Model

High-Fidelity Model

Subsonic, transonic, and supersonic aerodynamic force and moment data were obtained with an 8% scale sting-supported model

Received 20 December 1998; revision received 23 August 1999; accepted for publication 30 August 1999.

*Principal Engineer, Aerodynamics Department, Tactical Aircraft Programs. Senior Member AIAA.

†Unit Manager, Aerodynamics Department, Tactical Aircraft Programs.

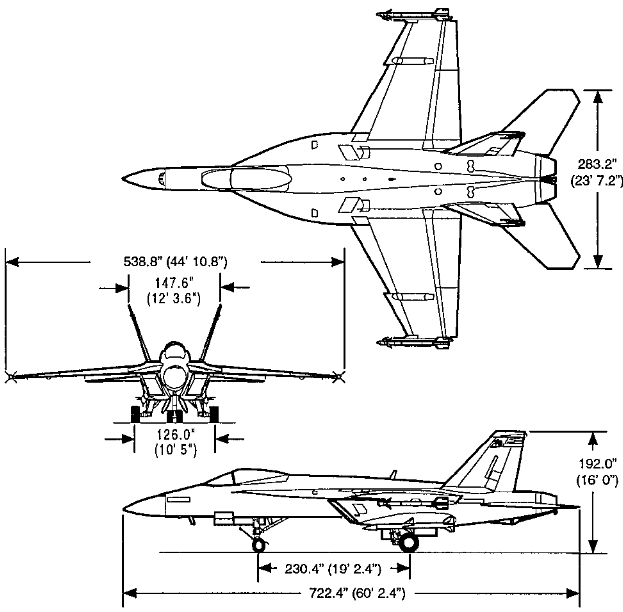

Fig. 1 F/A-18E three-view drawing.

Fig. 2 F/A-18E force and moment model, 8% scale.

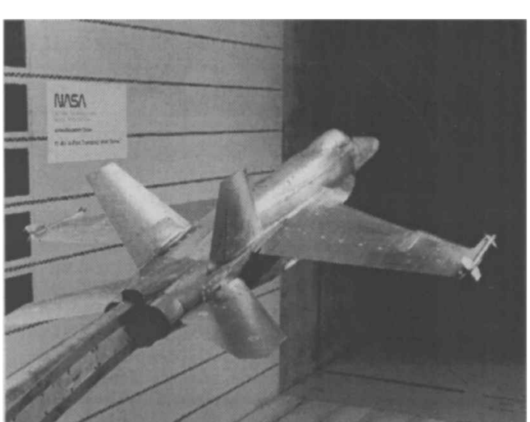

Fig. 3 F/A-18E model distorted afterbody, 8% scale.

(Fig. 2). The model was a complete configuration model with flow-through inlets and a distorted afterbody to accommodate the aft-support sting entry (Fig. 3). The model scale was selected to provide the largest model that would satisfy the interference criteria of the projected wind-tunnel facilities to be used for both baseline testing and testing with stores. The large size provided the opportunity to duplicate detailed moldline features including most protuberance items. The model also featured a full flowing inlet bleed system. All of the control surfaces had deflection capability. Single-piece control surface/attach brackets at numerous discrete deflections for the flaps, ailerons, rudders, and LEX spoiler were built for highly repeatable results.

Pretest Geometry Validation

Extensive moldline geometry validation was conducted for all test configurations with a coordinate measuring machine prior to testing to ensure the model was representative of the full-scale aircraft. All features found to be outside design tolerances were corrected prior to testing.

Single-Piece Balance Design

A single-piece, internal, six-component strain gauge balance was built for low-angle-of-attack testing, $\alpha \leq 12$ deg. It was designed specifically for the 8% scale force and moment model to provide highly accurate drag measurements. The standard deviation of the pretest calibration uncertainty was less than 0.1% of full-scale load. It also demonstrated more repeatable test results than past experience with multipiece balances. Intermediate and high-angle-of-attack testing was conducted with a multipiece, six-component, internal strain gauge balance to accommodate the larger load requirements.

Flow-Through Duct Design and Instrumentation

The model employed a total pressure rake in each duct as well as nozzle exit static pressure to determine duct forces and moments. The instrumentation was designed to allow data acquisition throughout the test due to the potential for external configuration changes to influence the duct pressures. A Labotto distribution was used to determine individual probe locations and area weighting factors for each rake. Prior to force and moment testing the duct and bleed instrumentation was calibrated in a nozzle thrust stand to obtain flow and thrust coefficients. Inserting laser-drilled plates of varying porosities into the duct controlled inlet mass flow. Screen mesh was not employed due to lack of repeatability. Duct exit chokes were not used due to the potential for varying base areas to influence afterbody pressures.

Diagnostic Pressure Instrumentation

Surface static pressure ports were installed on the model to confirm that wall interference was not influencing the results through comparison with CFD and tunnel-to-tunnel correlation. The pressure ports also provided correlation with the 15% sting and distortion/jet effects model and the aircraft, which were both instrumented with surface static pressures.

15% Sting and Distortion/Jet Effects Model

Pressure Model Approach for Afterbody Effects

Data acquired with the 8% scale force and moment model required adjustments to account for the effect of the support sting, the associated afterbody distortion, and the low-pressure, flow-through jet. A thorough study of available test techniques led to the design of the sting and distortion/jet effects model. A wing-tip support system was selected after several support-system options were evaluated (see Fig. 4, Table 1, and Ref. 2). High-pressure air for simulating jet flows was delivered to the model through the wing-tip mounting system. Pressure integration rather than a strain gauge balance was selected for increased measurement accuracy of afterbody force and moment increments (Table 2). This technique also provides information such as the extent of the sting and distortion/jet effects influence and pressure visualization through color contour plotting.

Fig. 4 Support system options.

Table 1 Support-system issues

Advantages	Disadvantages
Wing tip support	
Model and support blockage not severe	Some distortion of the wing section necessary
No support wake interference on afterbody	Zero or very small sideslip capability
Adequate variation in angle of attack obtainable	Support shock interference with afterbody
Established method	Choice of metric break restricted
Sting support	
No distortion of aircraft lines	Limited mass-flow capability particularly with cruise nozzle
Minimum blockage	Plume characteristics not correct
Lowest support interference on afterbody flow	Structurally limited
Some sideslip capability	Limited angle-of-attack capability
Freedom of choice of metric break	High cost separate supports for real and distorted afterbodies
	Difficult to route instrumentation leads
Strut support	
Only limited distortion of aircraft lines	Support wake and support shock interference with afterbody flow
Freedom of choice of metric break	Model and support blockage can be large
Established method	Variation in angle of attack not always possible
	No sideslip capability
	Negative past experience

Table 2 Force measurement issues

Force balance model	Pressure model
Balance uncertainty/repeatability	Pressure measurement uncertainty/ repeatability
Metric break effects	Leaking/plugged pressure identification
—Surface discontinuities	Incremental area definition
—Seal tares (different for real and distorted afterbody)	Bookkeeping areas and substitutions
Balance fouling	Adequate instrumentation in areas of steep pressure gradients
Cavity corrections	
—Area definition	
—Pressure measurement uncertainty/repeatability	
Balance shifts	
—Temperature gradients	

A model scale of 15% was selected to provide sufficient internal volume for the required onboard pressure instrumentation modules and air supply lines while avoiding wind-tunnel wall interference effects on the afterbody increments. Further discussion of this model can be found in Refs. 3–5.

High-Fidelity Model

The model featured interchangeable distorted and real afterbodies for sting and distortion testing (Fig. 5). The empennage control surfaces and all components forward of the afterbody were common to both configurations. The distorted afterbody configuration simulated the 8% force model, including flow-through ducts, duct rakes, sting cavity, and dummy sting. The real afterbody was representative of the aircraft including discretely variable exhaust nozzle geometry, nozzle pressure ratio control for jet effects testing, the environmental control system (ECS) heat exchanger exhaust with flow control, and engine bay vent (EBV) exhausts with flow control (Fig. 6).

Redundant Instrumentation for High-Risk Measurements

Early in the design stage, concern arose over the ability to successfully integrate pressures on the deflectable horizontal tail. Consequently, the left-hand tail was instrumented with a strain gauge balance that subsequently confirmed the accuracy of pressure integration on the right-hand pressure instrumental tail.

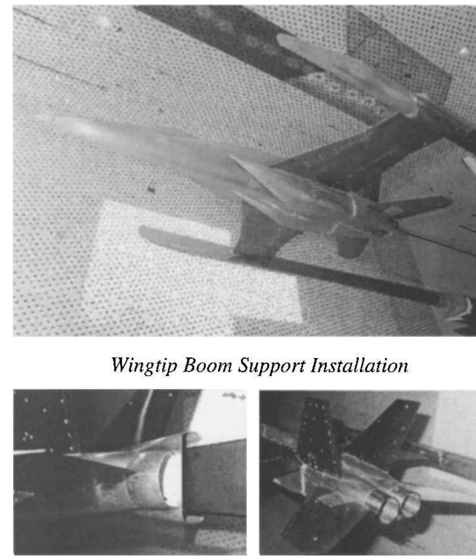

Wingtip Boom Support Installation

Distorted Afterbody *Real Afterbody*

Fig. 5 F/A-18E sting and distortion/jet effects model, 15% scale.

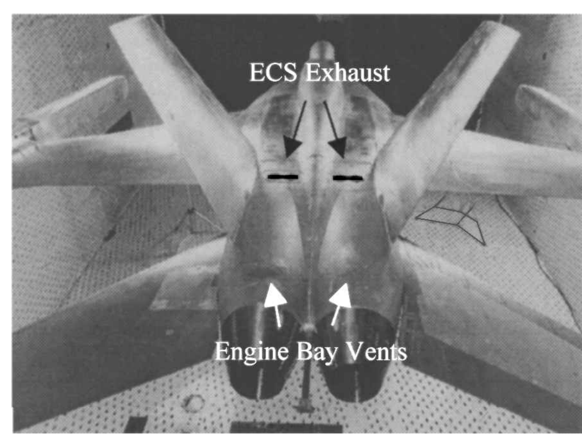

Fig. 6 Model configured with ECS and EBV exits.

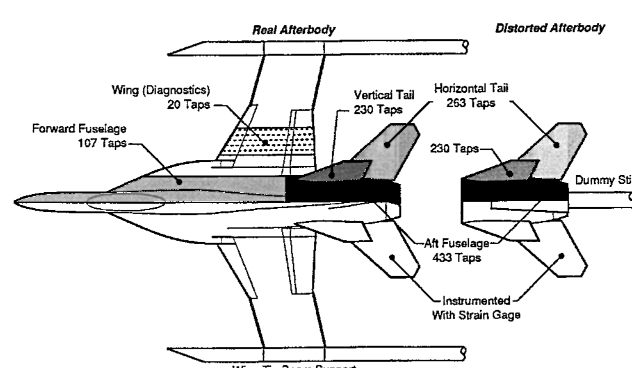

Fig. 7 Pressure tap distribution.

CFD for Locating Pressure Instrumentation

CFD results were used to determine the proper number and concentration of pressure taps required to accurately measure sting and distortion effects over the range of test conditions. Approximately 1050 pressure taps were distributed over the external surface of the model (Fig. 7). Pressure taps were concentrated in the afterbody region where sting and distortion and jet effects were predicted to be most pronounced. A sparse distribution of taps was included on the forward portion of the model to provide a closed body for pressure integration. This would minimize the effect of pressure instrumentation system bias on the results.

CFD for Model Development

Several additional CFD studies were performed to support the wind-tunnel model design effort. Euler analyses were conducted to aid in the design of an inlet fairing that would not impact the sting and distortion increments. This inlet fairing was then used in all subsequent computational and experimental studies. An Euler CFD study was performed to ensure that the design of the support booms and their wing-tip integration did not influence sting and distortion increments.

17.6% Integrated Inlet/Airframe Model

A high-fidelity, 17.6% scale inlet/airframe model was used for final preflight inlet performance testing (Fig. 8). This model incorporated both left and right flowing inlets, but only the left inlet was accurately modeled up to the aerodynamic interface plane, including a full bleed system representation. The model also featured removable forebody protuberances and the flight test noseboom to isolate their influence on inlet performance.

Force and Moment Accounting Procedure

Consistent Force and Moment Accounting Defined Early

The F/A-18E force and moment accounting procedure for the wind-tunnel-predicted aerodynamic and propulsion databases is illustrated in Fig. 9. All of the force components that are independent of engine power setting are included in the aircraft lift and drag characteristics. All of the factors that affect the engine cycle performance and all of the force components that are functions of engine throttle setting and exhaust system geometry are included in the installed propulsion system performance. The accounting procedure was developed at the outset of the wind-tunnel program planning effort to define the required test articles. The procedure was designed to identify and to track the fundamental force components in a consistent manner throughout the wind-tunnel and flight-test program. Components of the wind-tunnel force and moment accounting procedure were used to collapse flight-derived lift and drag to a set of aerodynamic reference conditions and to nominal test conditions as indicated by Fig. 9. The aerodynamic reference conditions are defined in Table 3.

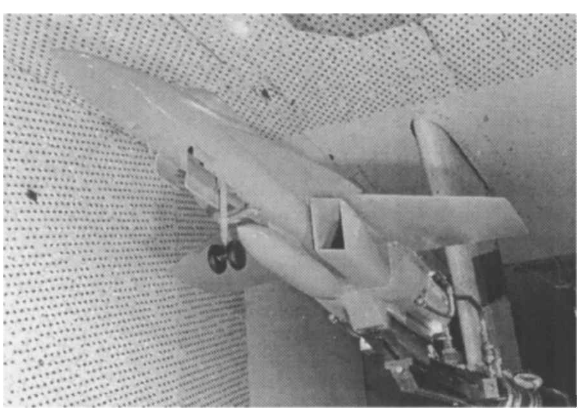

Fig. 8 Integrated inlet/airframe model, 17.6% scale.

Validation of Force and Moment Accounting Procedure

Test diagnostics were performed to validate the force accounting procedure by ensuring that there was no coupling of the spill drag and nozzle/afterbody drag effects. Examination of the 8% scale force model diagnostic pressure measurements confirmed that the influence of varying inlet mass flow was not observed in the afterbody pressure data. Examination of the 15% scale jet effects external pressures indicated that the nozzle/jet effects were limited to the afterbody and empennage surfaces. The 8% model inlet bleed flows were verified through comparison with the 17.6% integrated inlet/airframe test results. An evaluation of inlet spill induced lift and pitching moment concluded that these effects are negligible. Therefore, these elements are not included in the force and moment accounting procedure. Airframe flexibility effects were also found to negligible for the purpose of aircraft performance database development.

Table 3 Aerodynamic reference conditions

Aerodynamic influence	Reference condition
Inlet operation	Critical mass-flow ratio
Nozzle operation	Full open, exit static pressure ratio = 1.0
Center of gravity	25% of mean aerodynamic chord
Altitude	36,089 ft
Store load	Tip-mounted AIM-9 missiles (2)
Environmental control system	Mean operating drag level

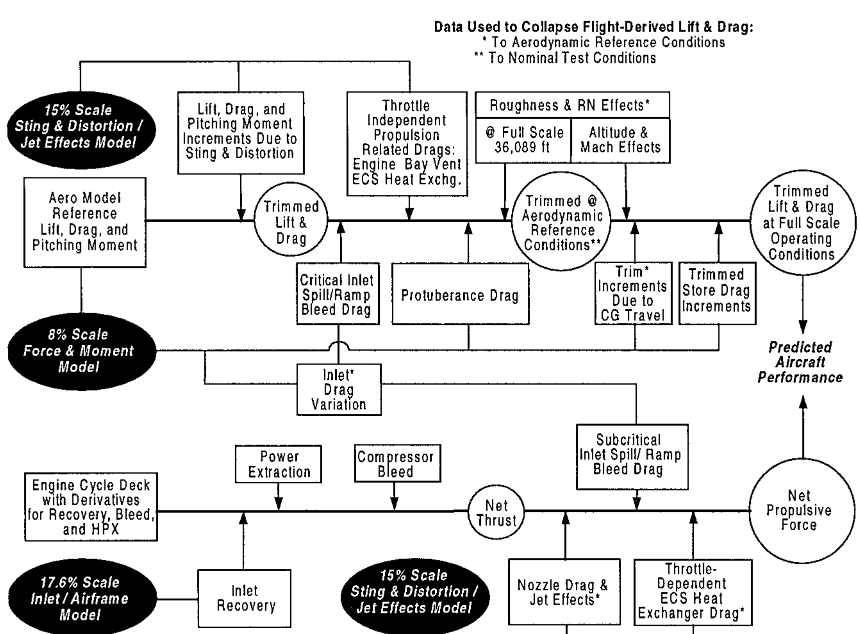

Fig. 9 Force and moment accounting procedure.

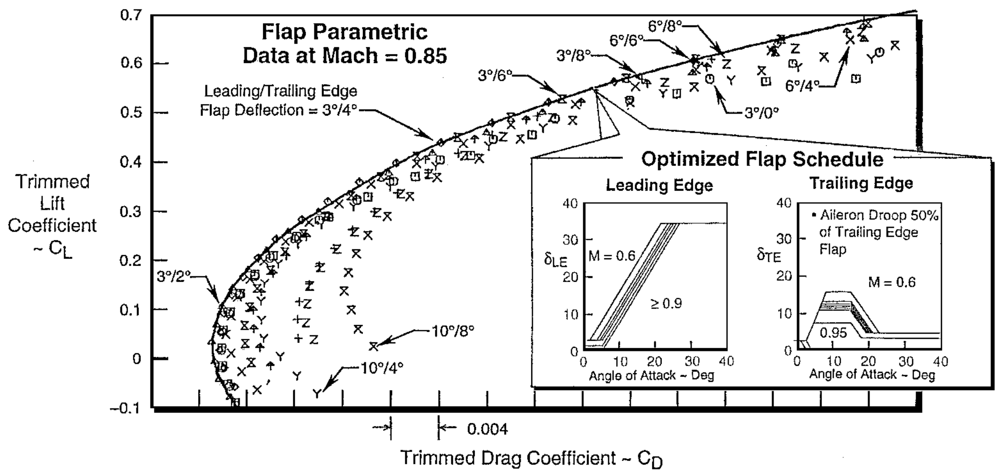

Fig. 10 Flap schedule optimized for minimum drag.

Wind-Tunnel Database Development

Force and Moment Testing

Large Interference-Free Test Facility

Force and moment testing was conducted with the 8% scale model in the NASA Ames Research Center 11-ft wind tunnel. Tunnel-wall effects were not evident in the test data as confirmed by CFD studies, tunnel-wall pressure measurements, test-to-test external pressure comparisons with a subsequent 8% scale entry in the Arnold Engineering Development Center (AEDC) 16T facility, and pressure comparisons with the 15% scale sting and distortion/jet effects model.

Strain Gage Balance Tailored to Angle-of-Attack/Load Range

To minimize force and moment data uncertainties, the NASA Ames Research Center 11-ft test was conducted in two phases to tailor balance selection to the expected load range. The first phase focused on low angle of attack and was conducted with the high-accuracy, single-piece balance. The balance and installation were changed for the second phase to accommodate the high load range requirements for intermediate to high angle of attack testing.

Extensive Control Surface Parametrics

Extensive flap, aileron, and horizontal tail parametrics were tested to accurately determine the induced drag characteristics. Flap hinges, actuator, and wingfold fairings were tested as part of the baseline configuration to account for their influence on induced drag during flap effect testing. Horizontal tail parametrics were performed at a select number of flap settings to incorporate the change in downwash caused by deflecting the trailing-edge flap and the resulting influence on tail effectiveness. The resulting trimmed fixed flap data was used to construct a minimum drag envelope, from which the flap schedules in the flight control system were developed (Fig. 10).

Test for Protuberance Impact

Tactical aircraft force and moment models typically do not simulate the protuberances of the full-scale aircraft. However, the drag increment due to these items is significant and must also be accounted for during database development. An extensive effort was made to identify and estimate the drag of all protuberance items. The design process included continuous tracking of all outer moldline protuberances to facilitate trade studies. There were 94 types of protuberances, resulting in a total of 386 individual protuberance items. The items included external fasteners of various types, which numbered 88,340, and skin panel gaps totalling 2,180 ft in length. Outer moldline surveys of production F/A-18C aircraft were used to determine the percentage of gaps that would be forward or aft facing. The large model scale permitted testing of the most significant protuberance items, Fig. 11. Seventy-one percent of the F/A-18E protuberance drag was based on wind-tunnel test data.

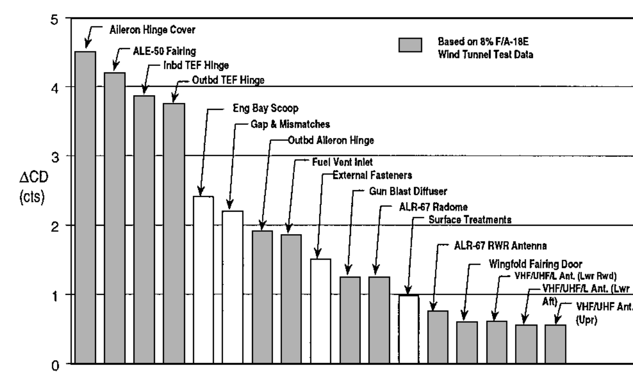

Fig. 11 Protuberance drag.

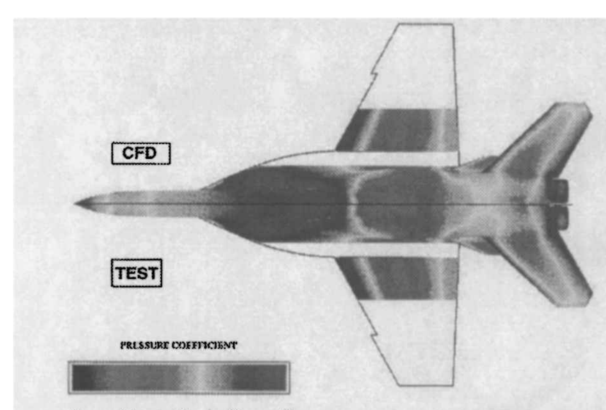

Fig. 12 Comparison of test and CFD predicted pressures.

Verification of Reynolds Number Effects

Reynolds number variation studies were performed during force and moment testing to confirm the analytical skin-friction drag methodology, over the range of available wind-tunnel data, that was used to adjust from wind-tunnel test conditions to full scale. Test Reynolds number varied from 3×10^6/ft to 8.6×10^6/ft. The latter value was approximately 34% of full scale at cruise conditions and was the highest that could be obtained due to facility operating limits for which the model was designed.

On-Line Flow-Through Duct Corrections

Internal duct forces and moments were determined for each test point using duct total pressure rakes and nozzle exit static pressures. This enabled the influence of individual configurations on the duct flowfield to be measured. Test results showed that external centerline store configurations and large stabilator deflections impacted duct performance.

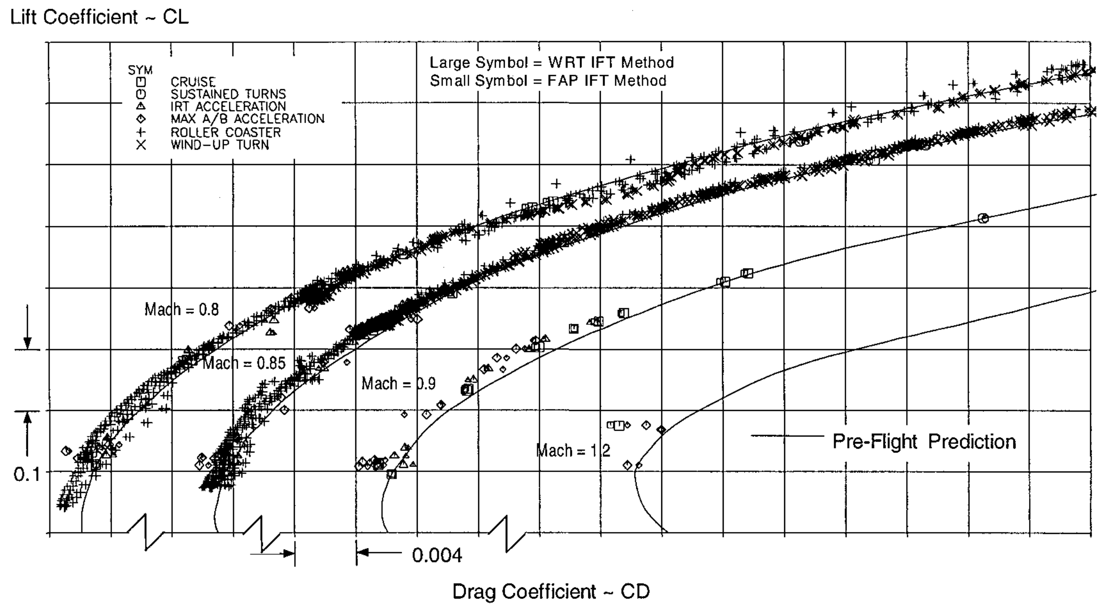

Fig. 13 F/A-18E2 flight-derived drag.

Sting and Distortion Testing

Large Interference-Free Test Facility

Sting and distortion testing was conducted in the AEDC 16T transonic wind tunnel. CFD studies verified that there were no apparent wall effects on the test results.

Tested for Secondary Influences on Sting and Distortion

The test program had several secondary objectives including the effects of fuselage missiles and control surfaces on the sting and distortion increments, EBV effects, and ECS heat exchanger exhaust effects. Data were obtained with a limited number of flap settings and horizontal tail deflections. Sting and distortion increments of lift, drag, and pitching moment as a function of control deflection were added to the basic aircraft untrimmed coefficients before trimming.

On-Line Correlation of CFD and Test Results

Continuous on-line monitoring of pressure and pressure-integrated force and moment results were available throughout the test. Three-dimensional surface pressure color contour displays that compared test and CFD results were monitored to assess data quality and to support elimination and substitution of faulty pressure measurements if necessary. On-line correlation of pretest Navier–Stokes CFD solutions and test data led to high confidence throughout the test (Fig. 12). A complete discussion of these test and CFD studies is provided in Refs. 3–5.

Wind-Tunnel–Flight Comparisons

The evaluation of flight-derived lift and drag is currently in progress based on two in-flight thrust determination techniques as discussed in a companion paper.[1] Although this evaluation is not complete, sufficient data have been acquired to conduct an initial correlation between wind-tunnel predictions and flight results. Flight-test results for the incremental lift and drag effects due to store carriage were not available at the time this paper was being prepared because this testing was just commencing. The following paragraphs present and discuss select aerodynamic and performance data to demonstrate the correlation between wind-tunnel and flight results.

The drag comparisons in Fig. 13 show the variation of drag with lift over a portion of the subsonic/supersonic flight envelope at the aerodynamic reference conditions. Flight data is provided for both in-flight thrust methodologies. Excellent agreement between wind-tunnel and flight results and between in-flight thrust methodologies is demonstrated. The flight data collapse very well for various altitudes, power settings, and maneuver types. This is an indication that the force and moment accounting system is valid, that the instrumentation systems are operating properly, that the data reduction procedures are operating properly, and that the maneuvers are conducted properly.

Conclusions

Development of a credible preflight database for accurate aircraft predictions requires commitment and resources. The success of the F/A-18E/F wind-tunnel program was a direct result of both of these. The commitment was made at the outset to develop and implement test techniques that would properly account for each item impacting aircraft performance either by wind-tunnel testing or by estimation. Adequate resources allowed the development of high-fidelity models, use of large, interference-free wind-tunnels, comprehensive test programs, and integration of CFD methods to ensure first-time quality test results. Front loading project resources to the wind-tunnel program were beneficial to the subsequent performance flight test program. The excellent agreement between wind-tunnel and flight results allowed the performance flight evaluation plan to be reduced by 60 flights and eliminated aircraft development flight testing for drag reduction as a result of optimistic predictions. The F/A-18E/F wind-tunnel program has demonstrated many successful wind-tunnel techniques that serves as a reference for future programs.

References

[1]Niewald, P. W., and Parker, S. L., "Flight Test Techniques Employed to Successfully Verify F/A-18E In-Flight Lift and Drag," AIAA Paper 99-0768, Jan. 1999.

[2]Hunt, B. L., and Gowadia, N. S., "Determination of Thrust and Throttle-Dependent Drag for Fighter Aircraft," AIAA Paper 81-1692, Aug. 1981.

[3]Hunter, K. J., Parker, S. L., and Niewald, P. W., "Experimental Determination of F/A-18E Afterbody Aerodynamics," AIAA Paper 99-0398, Jan. 1999.

[4]Bush, R. H., Jasper, D. W., Parker, S. L., Romer, W. W., and Willhite, P. G., "Computational and Experimental Investigation of F/A-18E Sting Support and Afterbody Distortion Effects," AIAA Paper 95-1779, June 1995.

[5]Willhite, P. G., Jasper, D. W., and Romer, W. W., "A Critical Evaluation of CFD Predictions of Full Aircraft Drag Increments," AIAA Paper 95-2289, June 1995.